SUPPLEMENT 1

Text S1

Sex identification

The Bermuda petrel shows some degree of sexual dimorphism in bill length with a mean of 28.3 mm (range: 27.3-29.6 mm, n = 14) for females and a mean of 30.09 mm (range: 29.1-31.2 mm, n = 21) for males (Brinkley & Sutherland 2020). Given the substantial overlap between measurements, we determined adult sex in the field by combining morphometric measurements (i.e., bill length and depth at gonys and body mass, Madeiros 2005) with cloacal examination after egg laying (Brinkley & Sutherland 2020). We also used molecular methods to sex 22 adult breeders (Fridolfsson & Ellegren 1999) from a few drops of blood collected with a capillary and stored in 100% ethanol until they were analysed in the laboratory.

References

Brinkley ES, Sutherland K (2020). Bermuda Petrel (Pterodroma cahow), version 2.0. In Birds of the World (Schulenberg TS, Keeney BK, Billerman SM, Editors). Cornell Lab of Ornithology, Ithaca, NY, USA. https://doi.org/10.2173/bow.berpet.02

Fridolfsson AK, Ellegren H (1999) A simple and universal method for molecular sexing of non-ratite birds. J Avian Biol 30:116–121 https://doi.org/10.2307/3677252

Madeiros J (2005) Recovery plan for the Bermuda petrel (Cahow) Pterodroma cahow. Department of Conservation Services, Hamilton

Text S2

GPS-logger retrieval rate and potential negative effect on bird body mass and breeding success

We examined the potential negative effects of tagging on foraging performance by comparing the change in body mass of tracked birds between logger deployment and logger retrieval, with the expectation of no change in mass (Bolt 2021). We first measured the body mass of 7 tagged birds (for which pre- and post-deployment weights were available) during the incubation (in 2019) when birds are easy to catch (at the nest) and when changes in bird body weight are not affected by chick feeding. We also compared the breeding success of 27 tagged birds (from incubation and chick-rearing) with that of 27 randomly selected individuals sampled in similar proportions to birds tagged in the four nesting-islands. Our analysis showed that the rate of GPS logger retrieval was higher during incubation on both years (2019: 100% N=23; 2022: 89%, N=18) compared to the chick-rearing phase (2019: 73% N=11; 2022: 85%, N=13). Moreover, in 2019, we verified that during incubation birds body mass after GPS logger retrieval was never below the pre-deployment value, (Paired t-test: t = 0.69, df = 6, p = 0.52) indicating that birds recovered the pre-deployment body mass and gained on average additional 7.3 g. Moreover, when we compared the breeding success of a subsample of tagged birds (N=27) with that of randomly selected control individuals (N=27) we found no significant difference (GLM: Estimate SE: 0.92 ±-0.57, Z= 1.60, *P*= 0.11).

Table S1. Individual information on tracked birds including trip start and end times, breeding phase, number of locations and number of trips per individual.

Bird_ID	Year	Start (GMT time)	End (GMT time)	Breeding phase	N.locs	N.trips
C0602	2019	05/02/2019 21:31	19/02/2019 14:31	Incubation	330	1
C0888	2022	03/02/2022 06:07	16/02/2022 20:07	Incubation	327	1
C0894	2022	07/02/2022 13:05	21/02/2022 15:05	Incubation	339	1
C1038	2022	06/02/2022 03:59	17/02/2022 07:59	Incubation	269	1
E0035	2019	04/02/2019 07:37	13/02/2019 01:37	Incubation	211	1
E0053	2022	11/02/2022 02:50	20/02/2022 22:50	Incubation	237	1
E0082	2019	02/02/2019 23:35	13/02/2019 15:35	Incubation	257	1
E0083	2022	03/02/2022 15:04	19/02/2022 21:04	Incubation	391	1
E0095	2019	07/02/2019 04:37	15/02/2019 15:37	Incubation	204	1
E0144	2019	04/02/2019 07:31	11/02/2019 16:31	Incubation	178	1
E0151	2019	07/02/2019 05:40	15/02/2019 22:40	Incubation	210	1
E0161	2019	03/02/2019 04:35	14/02/2019 12:35	Incubation	273	1
E0161	2022	03/02/2022 14:07	17/02/2022 22:07	Incubation	345	1
E0165	2019	08/02/2019 01:41	17/02/2019 18:41	Incubation	234	1
E0204	2022	07/02/2022 11:04	13/02/2022 02:04	Incubation	136	1
E0227	2019	05/02/2019 22:35	17/02/2019 23:35	Incubation	290	1
E0228	2019	05/02/2019 09:36	11/02/2019 17:36	Incubation	153	1
E0231	2022	03/02/2022 02:00	05/03/2022 20:59	Incubation	528	2
E0289	2019	10/02/2019 02:33	23/02/2019 19:33	Incubation	330	1
E0323	2019	04/02/2019 22:30	20/02/2019 16:30	Incubation	379	1
E0362	2019	09/02/2019 21:37	21/02/2019 08:37	Incubation	276	1
E0362	2022	09/02/2022 06:04	20/02/2022 22:04	Incubation	281	1
E0376	2019	06/02/2019 08:37	18/02/2019 03:37	Incubation	284	1
E0401	2019	31/01/2019 03:45	12/02/2019 23:45	Incubation	309	1
E0423	2022	06/02/2022 05:00	17/02/2022 22:00	Incubation	282	1
E0481	2022	09/02/2022 03:06	24/02/2022 04:06	Incubation	362	1
E0546	2022	09/02/2022 04:00	17/02/2022 03:00	Incubation	192	1
E0636	2022	06/02/2022 08:02	15/02/2022 18:02	Incubation	227	1
C0894	2022	24/03/2022 04:00	28/03/2022 03:00	Early chick-rearing	96	1
E0171	2019	29/03/2019 07:31	04/04/2019 16:31	Early chick-rearing	154	1
E0171	2022	21/03/2022 13:04	29/03/2022 03:04	Early chick-rearing	183	1
E0196	2019	29/03/2019 04:31	02/04/2019 15:31	Early chick-rearing	108	1
E0197	2022	19/03/2022 06:00	23/03/2022 20:00	Early chick-rearing	111	1
E0212	2022	21/03/2022 01:45	28/03/2022 08:45	Early chick-rearing	176	1
E0243	2019	30/03/2019 05:03	05/04/2019 21:03	Early chick-rearing	161	1
E0243	2022	18/03/2022 07:30	22/03/2022 23:30	Early chick-rearing	113	1
E0252	2022	22/03/2022 09:00	27/03/2022 21:00	Early chick-rearing	133	1
E0362	2019	29/03/2019 05:31	07/04/2019 17:31	Early chick-rearing	229	1
E0363	2019	03/04/2019 07:02	10/04/2019 00:02	Early chick-rearing	162	1
E0368	2019	29/03/2019 06:03	06/04/2019 01:03	Early chick-rearing	188	1
E0434	2022	19/03/2022 05:00	27/03/2022 20:00	Early chick-rearing	208	1
E0526	2022	18/03/2022 10:30	21/03/2022 19:30	Early chick-rearing	82	1
E0537	2022	17/03/2022 08:30	24/03/2022 21:30	Early chick-rearing	182	1
E0552	2019	31/03/2019 08:30	06/04/2019 01:30	Early chick-rearing	138	1

Text S3

Analytical details on discrete-time Hidden-Markov-Models (HMMs)

The data streams used by the HMM to infer the behavioural states of the animals along each movement step are the step length (i.e. ground speed) and turning angle. Prior to fitting the HMM to the data, we specified that we wanted the model to classify the movement steps into two states: transit vs searching. To do so, we indicated that the "transit" steps would be characterised by high speed and high movement directionality. The searching state would be characterised by lower ground speed. To do so, we provided the following initial probability distribution parameters: step length from a Gamma distribution (mean = 30 kmh^{-1}, sd = 20 kmh^{-1}); turning angle from a wrapped Cauchy (concentration = 0.1). The search steps initial probability distribution parameters were instead: step length from a Gamma distribution (mean = 10 kmh^{-1}, sd = 20 kmh^{-1}); turning angle from a wrapped Cauchy (concentration = 0.1). As other mesopelagic predators were found to maintain a relatively high movement directionality also when searching for food (Ventura et al. 2022), we adopted a conservative approach and chose to specify the same concentration parameters as initial values for both "transit" and "search". The estimated state-specific step length and turning angle estimated by the model are shown below in Fig S1.
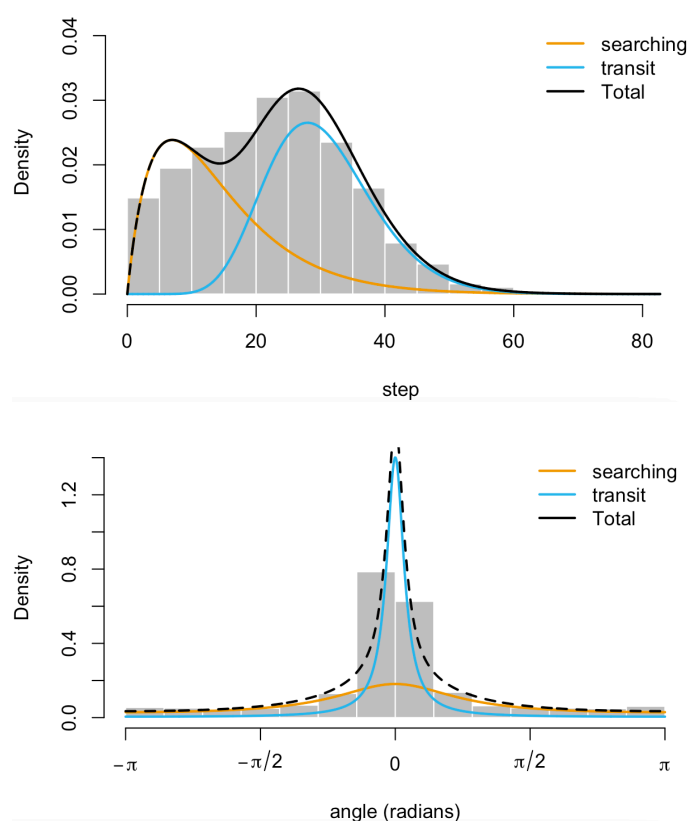
Fig. S1. Density distributions of the state-specific step length and turning angle estimated by the *Hidden-Markov-Models* for the Bermuda petrels.
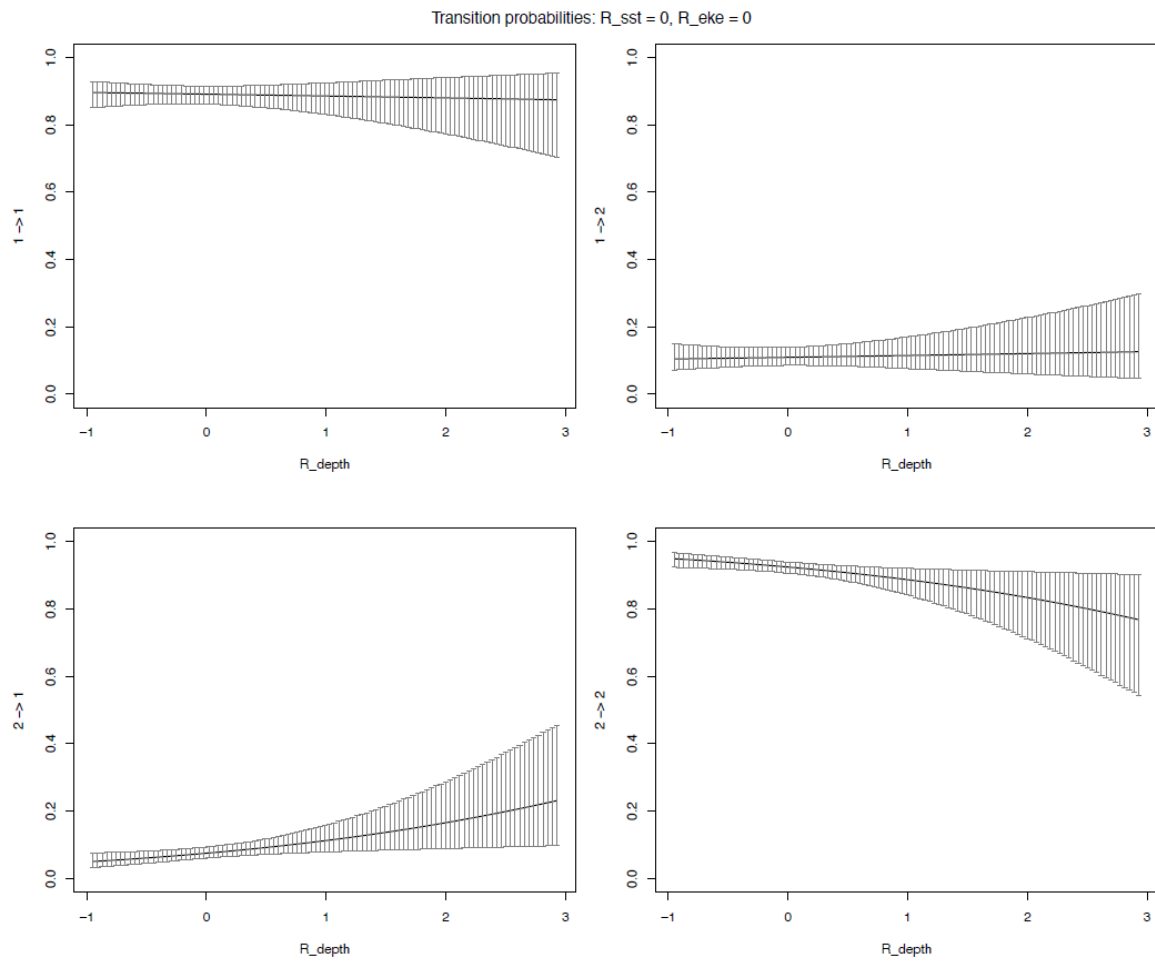
Text S4

Results of HMMs

The best HMM for the incubation dataset retained depth, SST, wind intensity and EKE as significant predictors of the probabilities of state switching. Specifically, the probability of switching from transit to searching was higher in shallower and cooler waters characterised by higher EKE. Switching from searching to transit was more likely when birds experienced stronger winds. During chick-rearing, the best HMM retained depth, SST and EKE as significant explanatory variables affecting state-switching. Specifically, switching from transit to searching was more likely in shallower waters while switching from searching to transit was more likely in warmer waters characterised by lower EKE. However, compared to a null model without environmental covariates affecting the state switching probabilities, the inclusion of explanatory variables only affected the final behavioural classification marginally: overall, only 1.4% of the total locations changed state after the inclusion of habitat covariates for both incubation and chick-rearing tracks. See Figs. S2 & S3 as examples.

Figures below are two examples showing the effect of sea surface temperature gradient (SSTgrad =sstslope) and depth respectively on the behavioural classification (made by means HMM) of "search" and "transit" states. Transition probability (1 = transit and 2 = search) for each combination of behavioural state is presents below.
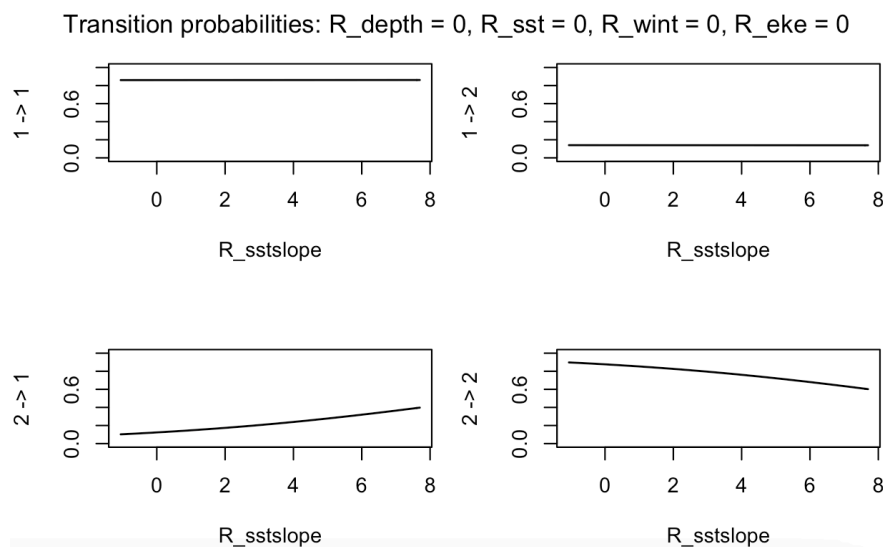
Fig. S2. Effect of sea surface temperature gradient (SSTgrad =sstslope) on the behavioural classification (made by means HMM) of "search" and "transit" states. Transition probability (1 = transit and 2 = search) for each combination of behavioural state.

Fig. S3. Effect of depth on the behavioural classification (made by means HMM) of "search" and "transit" states. Transition probability (1 = transit and 2 = search) for each combination of behavioural state.

Text S5

Stable Isotope Analysis details

Stable Isotope Analysis (SIA) of animal tissues provides a powerful tool to characterize seabird use of trophic resources and their role within marine food webs (Michener & Kaufman 2007). Naturally occurring nitrogen ($^{15}N/^{14}N$, $\delta^{15}N$) and carbon ($^{13}C/^{12}C$, $\delta^{13}C$) isotopic forms are assimilated through diet, fractioned and incorporated into tissues as these are formed (Hobson 1999). Consequently, consumers are enriched in ^{15}N in a predictable manner relative to their food and $\delta^{15}N$ measurements serve as indicators of a consumer diet and trophic level (Vanderklift & Ponsard 2003). In the marine food webs, $\delta^{15}N$ values show a stepwise increase from one trophic level to the next, with typical enrichment of about 3% per trophic level (Post 2002). Conversely to $\delta^{15}N$, stable carbon $\delta^{13}C$ values vary little along the food chain and $\delta^{13}C$ ratios are mostly used to determine sources of primary production supporting food web components (Kelly 2000), indicating inshore versus offshore foraging habitats, or pelagic versus benthic contributions to food intake (Hobson et al. 1994).

$\delta^{13}C$ and $\delta^{15}N$ values in the samples were determined by continuous flow isotope mass spectrometry (CF-IRMS) (Preston & Owens 1983), on a Sercon Hydra 20-22 (Sercon, UK) stable isotope ratio mass spectrometer, coupled to a EuroEA (EuroVector, Italy) elemental analyzer for online sample preparation by Dumas-combustion. Delta Calculation was performed according to $\delta X = [(R_{sample}/R_{standard}) -1] \times 1000$, where X is ^{13}C or ^{15}N and R_{sample} is the corresponding ratio of the heavy isotope to light isotope ($^{13}C/^{12}C$ or $^{15}N/^{14}N$). The reference materials used were Protein Standard OAS/Isotope and Sorghum Flour Standard OAS/Isotope (Elemental Microanalysis, UK), and IAEA-N1 for carbon and nitrogen isotope ratio (with, respectively, $\delta^{13}C$-26.98+/-0.13‰ Vienna Pee Dee Belemnite (VPDB) (Protein Standard OAS/Isotope), $\delta^{13}C$-13.68+/-0.19 VPDB (Sorghum Flour OAS), $\delta^{15}N$ +5.94+/-0.08 AIR (Protein Standard OAS/Isotope), $\delta^{15}N$ +0.4+/-0.2 AIR (IAEA-N1)). Uncertainty of the isotope ratio analysis, calculated using values from 6 to 9 replicates of isotopic reference material (Protein Standard OAS/Isotope, $\delta^{15}N$ +5.94+/-0.08 AIR, $\delta^{13}C$ -26.98+/-0.13‰ VPDB interspersed among samples in every batch analysis, was ≤ 0.1‰. The major mass signals of N and C were used to calculate total N and C abundances, using Protein Standard OAS (Elemental Microanalysis, UK, with 1.47%N, 46.26%C and 1.47%N, 39.53%C respectively) as elemental composition reference material.

References

Hobson KA (1999) Tracing origins and migration of wildlife using stable isotopes: a review. Oecologia 120:314 –326 https://doi.org/10.1007/s004420050865

Hobson KA, Piatt JF, Pitocchelli J (1994) Using Stable Isotopes to Determine Seabird Trophic Relationships. J Anim Ecol 63:786:798 https://doi.org/10.2307/5256

Kelly JF (2000) Stable isotopes of carbon and nitrogen in the study of avian and mammalian trophic ecology. Can J Zool 78:1-27 https://doi.org/10.1139/z99-165

Michener RH, Kaufman L (2007) Stable isotope ratios as tracers in marine food webs: an update. In Michener R & Lajtha K (eds) Stable isotopes in ecology and environmental science. Malden, MA:Blackwell Publishing, pp. 238–282

Preston T, Owens N (1983) Interfacing an automatic elemental analyser with an isotope ratio mass spectrometer: the potential for fully automated total nitrogen and nitrogen-15 analysis. The Analyst 108:971

Vanderklift MA, Ponsard S (2003) Sources of variation in consumer-diet delta 15N enrichment: a meta-analysis. Oecologia. 136:169-82 https://doi.org/10.1007/s00442-003-1270-z

Text S6

Prey species identification

DNA isolation

DNA was isolated with Norgen Stool DNA isolation kit, following the recommended protocol. For samples with more than 200 mg, we used 1 to 3 extraction replicates. DNA was eluted in 70 µL of elution buffer preheated at 70ºC and incubated at room temperature for 30 min before centrifuging. DNA from replicates was combined and each sample was then concentrated by evaporation with SpeedVac or precipitated with 3M Sodium Acetate to a final volume of 20 µL. The final DNA concentration was measured with Qubit 2.0 (Invitrogen). Two samples had no detectable DNA and the remaining were used for DNA metabarcoding, with concentrations ranging 0.2 – 7 ng/µL for faeces and 40 ng/µL for regurgitates.

DNA metabarcoding

DNA metabarcoding library preparation and sequencing were carried out by AllGenetics & Biology SL (www.allgenetics.eu). Libraries were prepared to target the main prey groups, fishes and cephalopods, with gene fragments from 16S and COI. A combination of primers from Deagle et al. (2009) was used to amplify the 16S gene (Chord_16S_F/Chord_16S_R for fish and Ceph_16S_F / Ceph_16S_R for cephalopods). Primers used to amplify the COI gene were mlCOIintF/ jgHCO2198 from Leray et al. (2013).

Blocking primers to prevent host DNA amplification were designed by AllGenetics following Vestheim and Jarman (2008) using Geneious 11.1.5 (Biomatters Ltd): 5' CCTGTGGAACTTAAAAATCAGCRACCACC 3' for the 16S region and 5' CTGTATACCCTCCTCTAGCAGGCAATCTAG 3' for the COI region. A C3 CPG spacer was added to the 3' end of each blocking primer to prevent elongation.
PCRs were carried out in a final volume of 25 µL, containing 2.5 µL of template DNA, 0.5 µM of the primer, Blocking Primer 20:1, 6.25 µL of Supreme NZYTaq 2x Green Master Mix (NZYTech, 0.5x final concentration), CES 1x, and ultrapure water up to 25 µL. Primers included the Illumina sequencing primer sequences attached to their 5' ends. The reaction mixture was incubated as follows: an initial denaturation step at 95 ºC for 5 min, followed by 35 cycles of denaturing at 95 ºC for 30 s, annealing temperature of 51 ºC for COI and 48 º C for 16S for 45 s, elongation at 72 ºC for 45 s, and a final extension step at 72 ºC for 7 min.
Only regurgitate samples were successfully amplified for both COI and 16S. Because amplification of COI under these conditions was suboptimal for most samples, conditions were optimized to a final volume of 12.5 µL, with a 1.23x final concentration of Supreme NZYTaq 2x Green Master Mix (NZYTech), Blocking Primer 15:1, 0.5 µM of each primer, CES 1x and 3.5 mM of $MgCl_2$. The most concentrated samples were diluted to 1:10 and 2.5 µL of the diluted DNA was added to the reaction. Eight faecal samples were also amplified with these conditions for COI and were subsequently sequenced. None of the faecal samples amplified for the 16S gene.
The oligonucleotide indices which are required for multiplexing different libraries in the same sequencing pool were attached in a second PCR round with identical conditions but only 5 cycles and 60 ºC as the annealing temperature. A negative control that contained no DNA was included in every PCR round to check for contamination during library preparation.

Libraries were purified using the Mag-Bind RXNPure Plus magnetic beads (Omega Biotek) and pooled in equimolar amounts according to the quantification with Qubit dsDNA HS Assay (Thermo Fisher Scientific) and sequenced in 1GB of NovaSeq PE250 (Illumina)

Sequence analysis and taxonomic assignment

FASTQ data was processed under Qiime2-2021.4 pipeline (Bolyen et al. 2019) with DADA2 plugin (Callahan et al. 2016) to denoise and dereplicate paired-end sequences. Trimming thresholds were set to cut the primers at the 5' end and low quality bases at the 3' end. Reads were truncated at the first base with Phred quality score equal or lower than 20. Sequences were classified with Qiime2 classify-consensus-vsearch (Bokulich et al. 2018, Rognes et al. 2016) using the Midori database as reference (Machida el al. 2017), setting 0.75 as minimum identity. Unassigned and non-prey sequences were discarded and classification was repeated with 0.9 of minimum identity for COI gene. We retained likely species with identity values >0.9. However, for the 16S gene final data set, retained prey species had homology values between 94% (only one out of the 12 identified species) and 99% (n=6 out of 12). Regarding the COI gene, retained prey species had homologies that varied between 99 and 100% (only three of the 14 identified species had homologies of 99%). Prey classification was confirmed with online NCBI blastN and adjusted to the least common ancestor if other taxa were assigned with similar identity or if the species had no documented occurrence in the North Atlantic.

References

Bokulich NA, Kaehler BD, Rideout JR et al. (2018) Optimizing taxonomic classification of marker-gene amplicon sequences with QIIME 2's q2-feature-classifier plugin. *Microbiome* 6:90. doi: 10.1186/s40168-018-0470-z

Bolyen E, Rideout JR, Dillon MR et al. (2019) Reproducible, interactive, scalable and extensible microbiome data science using QIIME 2. *Nature Biotechnology* 37:852–857. doi: 10.1038/s41587-019-0209-9

Callahan BJ, McMurdie PJ, Rosen MJ, Han AW, Johnson AJA, Holmes SP (2016) Dada2: high-resolution sample inference from illumina amplicon data. Nature methods, 13(7):581. doi:10.1038/nmeth.3869.

Deagle BE, Kirkwood R, Jarman SN (2009) Analysis of Australian fur seal diet by pyrosequencing prey DNA in faeces. *Molecular Ecology*, 18: 2022-2038. doi: 10.1111/j.1365-294X.2009.04158.x

Leray M, Yang JY, Meyer CP, Mills SC, Agudelo N, Ranwez V, Boehm JT, Machida RJ (2013) A new versatile primer set targeting a short fragment of the mitochondrial COI region for metabarcoding metazoan diversity: application for characterizing coral reef fish gut contents. *Frontiers in Zoology* 10**,** 34. https://doi.org/10.1186/1742-9994-10-34

Machida RJ, Leray M, Ho SL, Knowlton N (2017) Metazoan mitochondrial gene sequence reference datasets for taxonomic assignment of environmental samples. *Scientific Data* 4, 170027. doi: 10.1038/sdata.2017.27

Rognes T, Flouri T, Nichols B, Quince C, Mahé F (2016) Vsearch: a versatile open source tool for metagenomics. PeerJ, 4:e2584. doi:10.7717/peerj.2584.

Vestheim H, Jarman SN (2008) Blocking primers to enhance PCR amplification of rare sequences in mixed samples - a case study on prey DNA in Antarctic krill stomachs. *Frontiers in Zoology* 5: 12. doi: 10.1186/1742-9994-5-12.
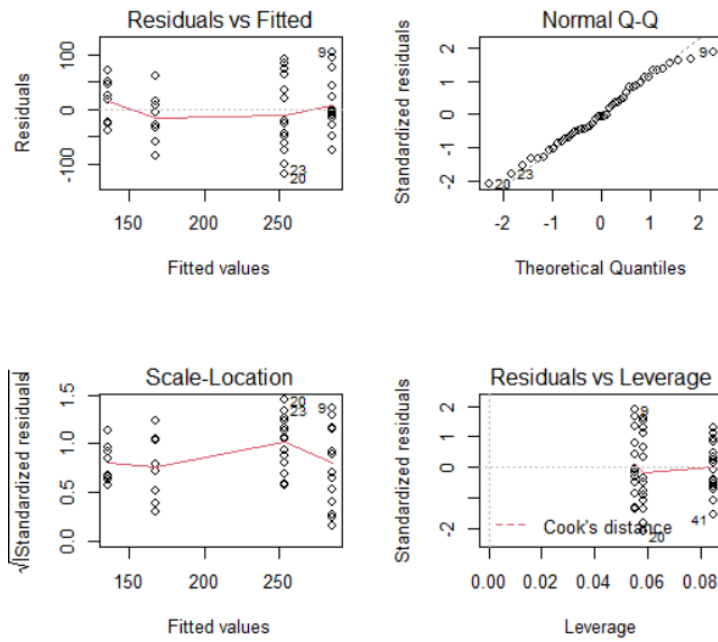
ANOVA residual plots applied to Bermuda petrel trip metrics (both years grouped) presented in Table 1. Note that Speed foraging was analysed using non-parametric Aligned Rank Transformation ANOVA.
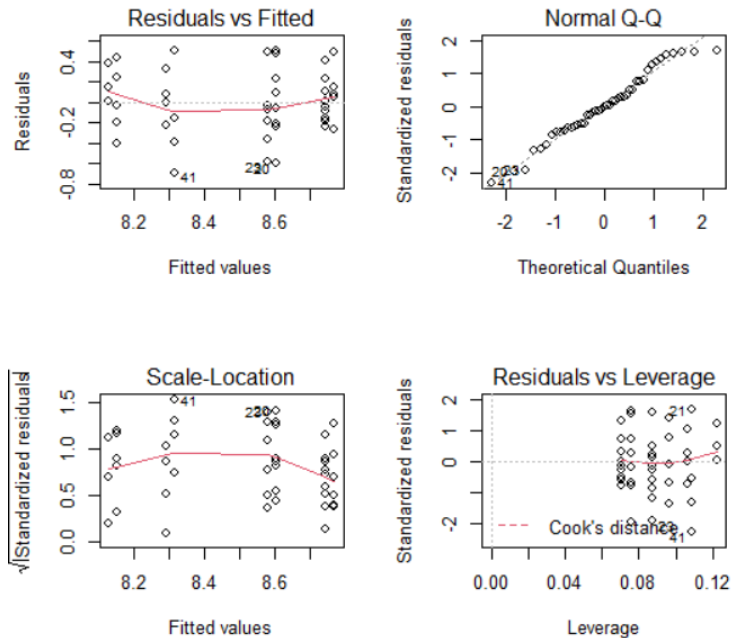
Fig. S4. ANOVA residual plots of log-transformed (Total distance)
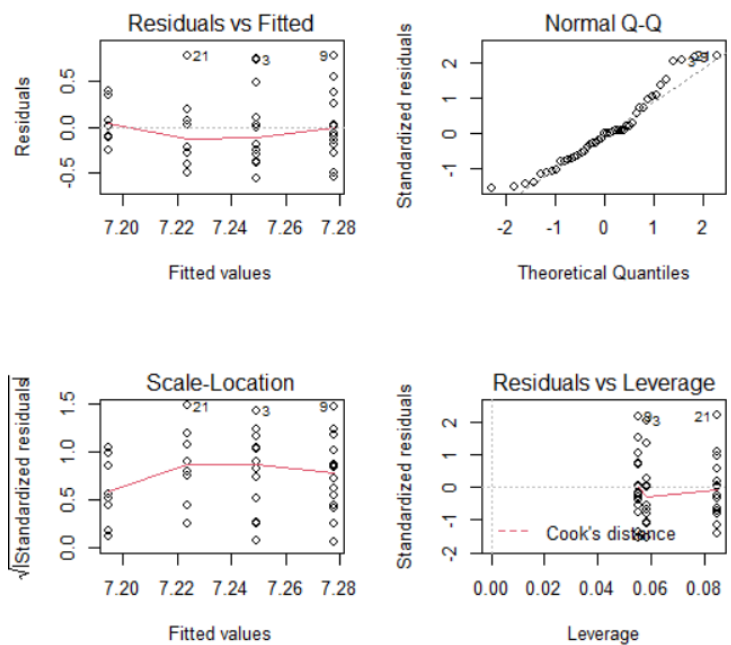
Fig. S5. ANOVA residual plots of log-transformed (Maximum distance)

Fig. S6. ANOVA residual plots of trip duration
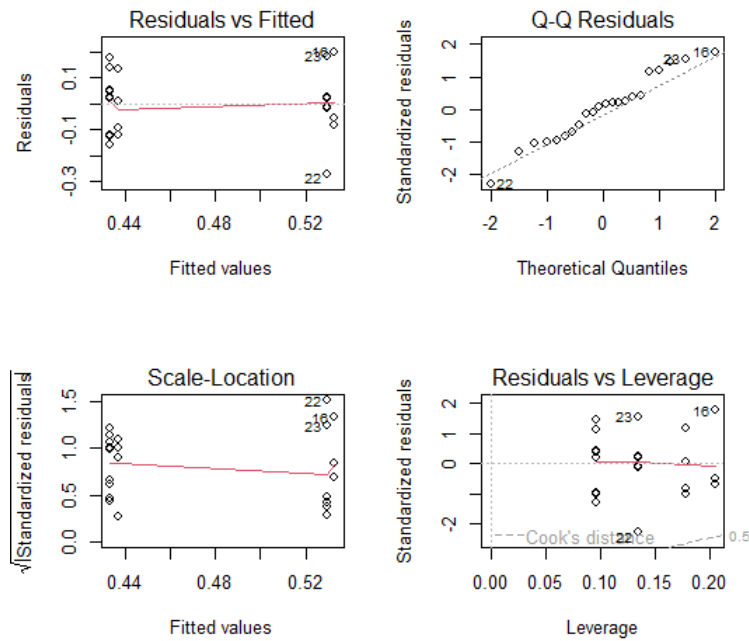
Fig. S7. ANOVA residual plots of proportion of time foraging (2019)
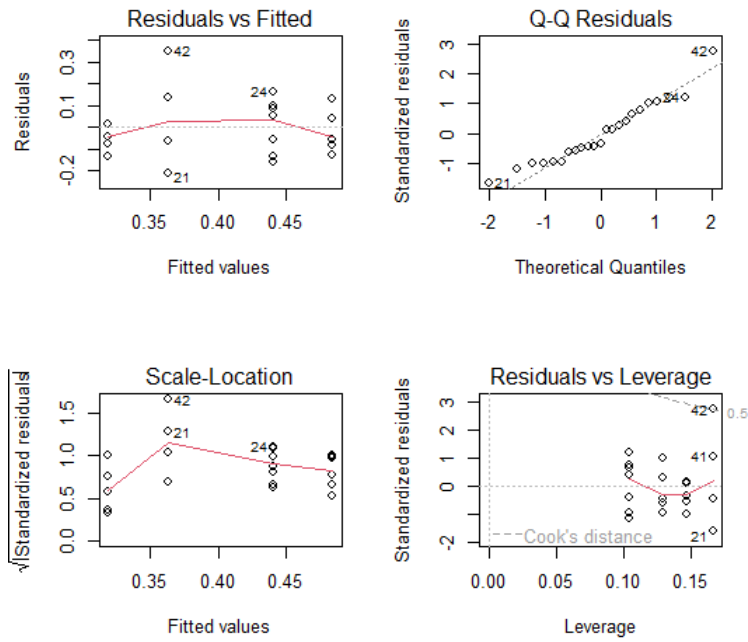
Fig. S8. ANOVA residual plots of the proportion of time foraging (2022)
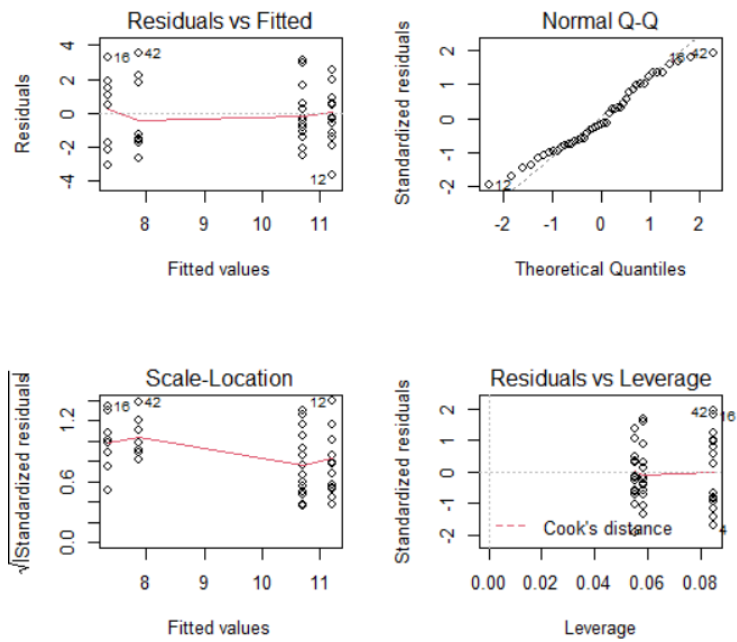
Fig. S9. ANOVA residual plots of Square root-transformed (Time foraging).
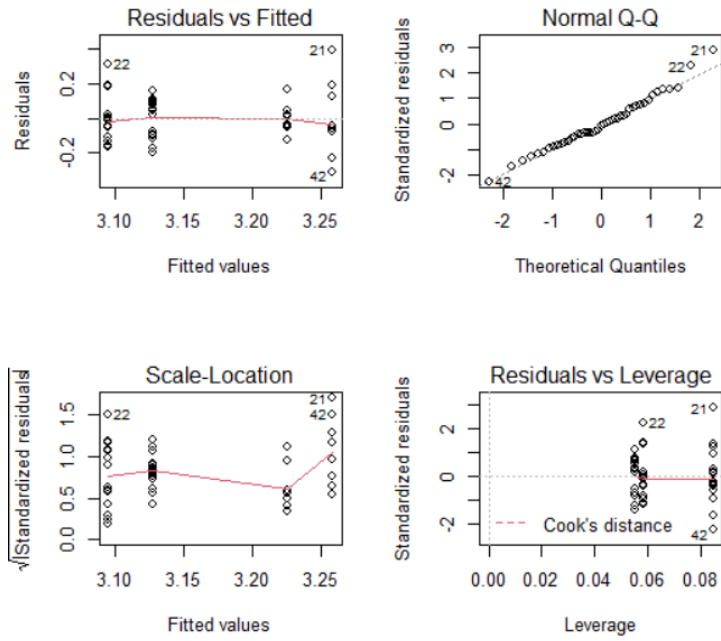
Fig. S10. ANOVA residual plots of log-transformed (Speed).
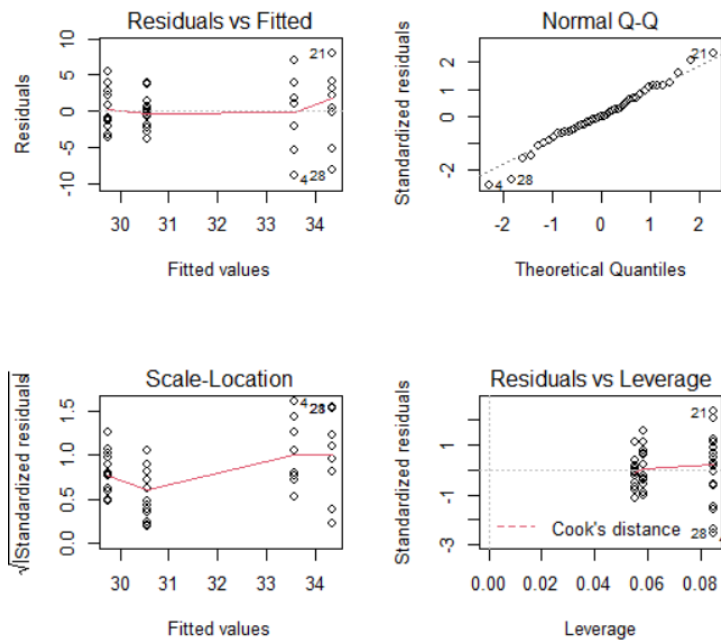
Fig. S11. ANOVA residual plots of speed travelling

Table S2 Summary of habitat variables tested as predictors of foraging habitat preferences. Locations (from 52 foraging trips). Mean±SD values and range are shown for those classified as "search" by HMM and used as proxy putative foraging behaviour and presented according to the incubation and early chick-rearing phases.

| Habitat characteristics	Incubation	Early chick-rearing
Depth foraging (m)	4845±692	3956±1347
range	4255-5193	1132-5107
Slope foraging (°)	1.5±0.7	1.6±1.5
range	0.5-4.6	0.5-6.5
SST foraging (°C)	19.0±1.3	13.6±4.6
range	15.2-21.0	3.8-18.8
SSTgrad (°)	0.002±0.002	0.003±0.002
range	0.001-0.004	0.002-0.003
SLA (m)	0.06±0.23	0.02±0.19
range	-0.07 – 0.13	-0.15 – 0.19
EKE (m^2s^{-2})	0.19±0.23	0.11±0.17
range	0.05-0.41	0.018-0.191
Chlorophyll a (mgm^{-3})	0.174±0.079	0.560± 0.588
range	0.076-1.40	0.043- 4.29
Wind speed (kmh^{-1})	37.4±13.8	34.2±13.4
range	27.7- 41.9	28.0-38.7
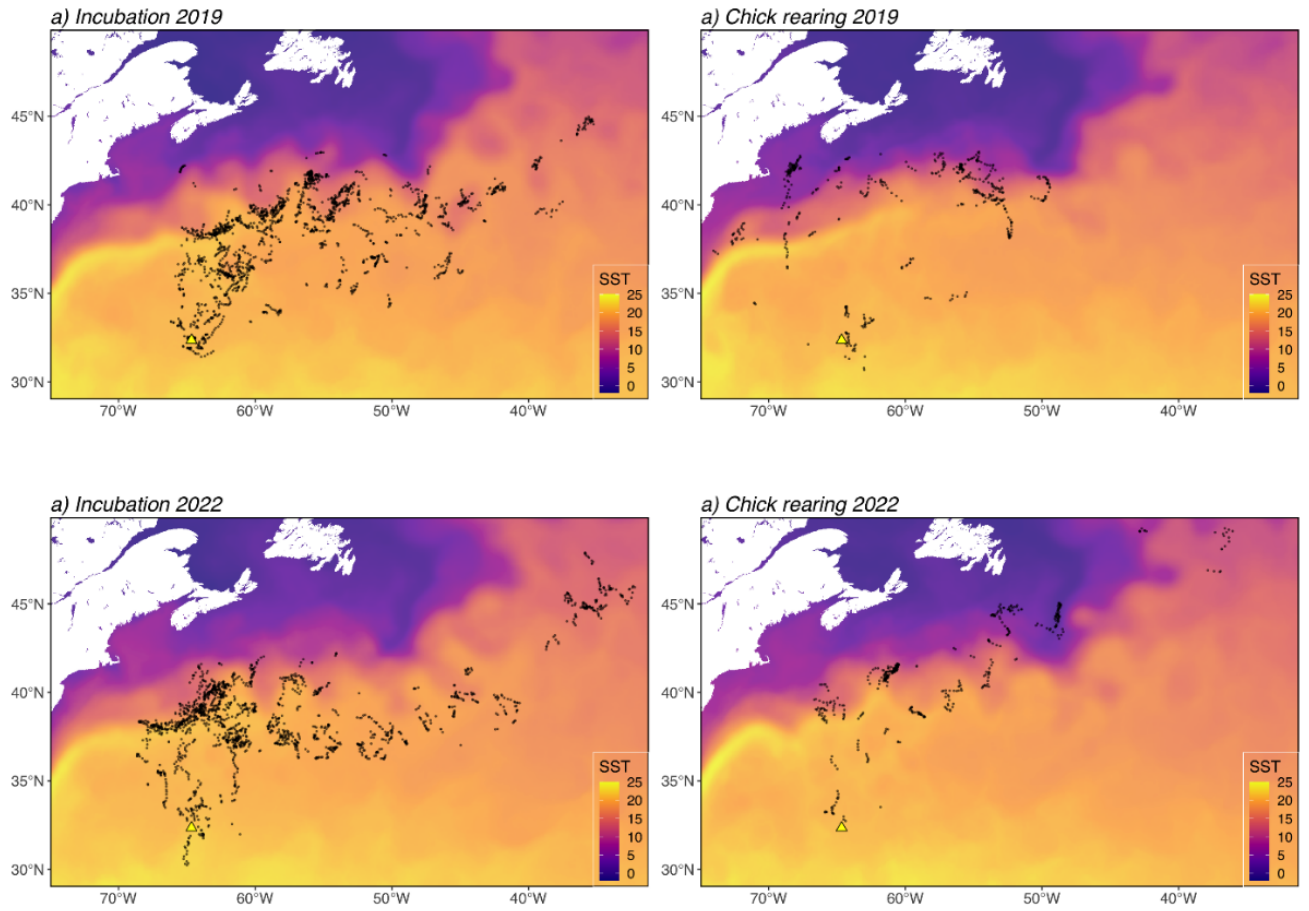
Fig. S12. "Search" locations classified by means HMM (see Methods for more details) along Bermuda petrel foraging trips and superimposed to mean SST layers presented by breeding phase and year.
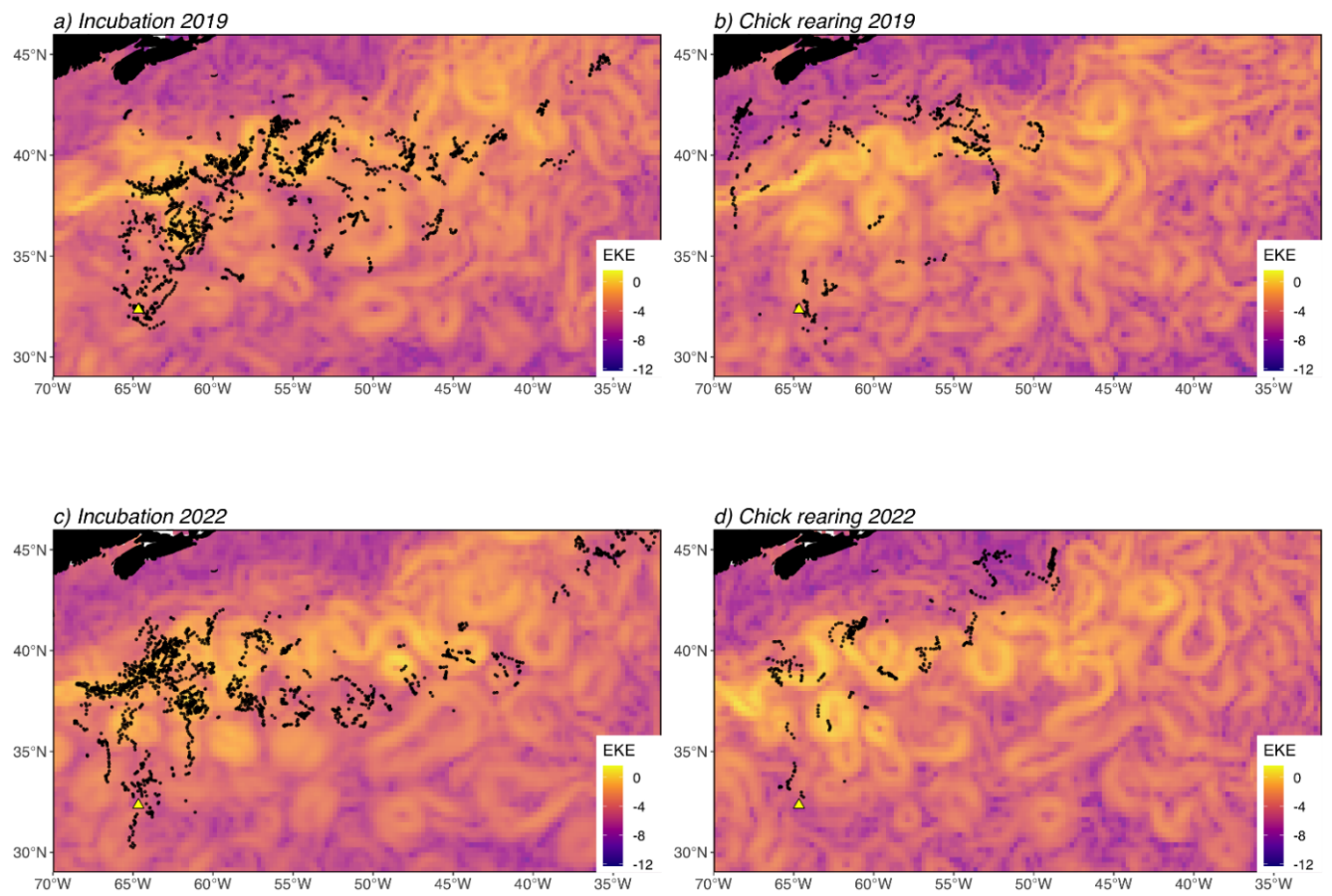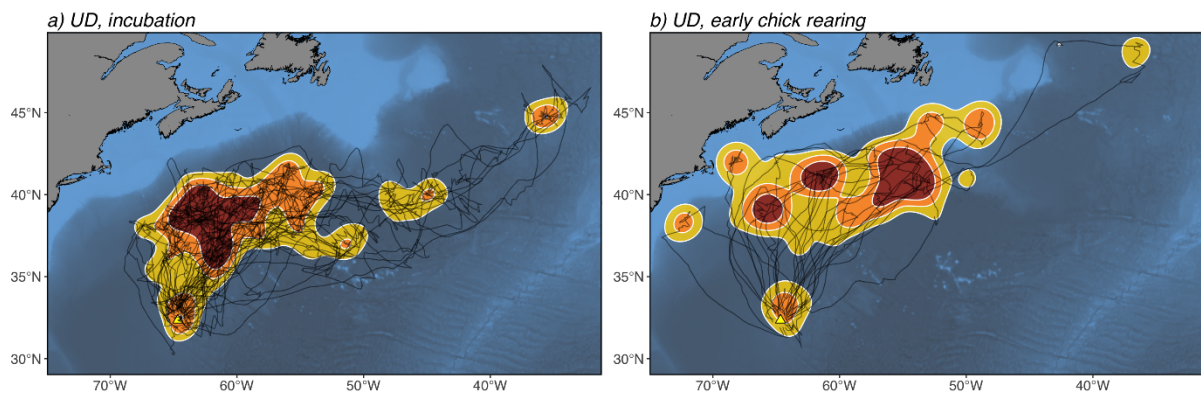
Fig. S13. Bermuda petrel locations classifies as "search" by means HMM (see Methods for more details) overlaid to the layer representing Eddy Kinetic Energy (EKE) in the western North Atlantic during the study period. EKE was used as a surrogate of mesoscale activity (warmer colours).
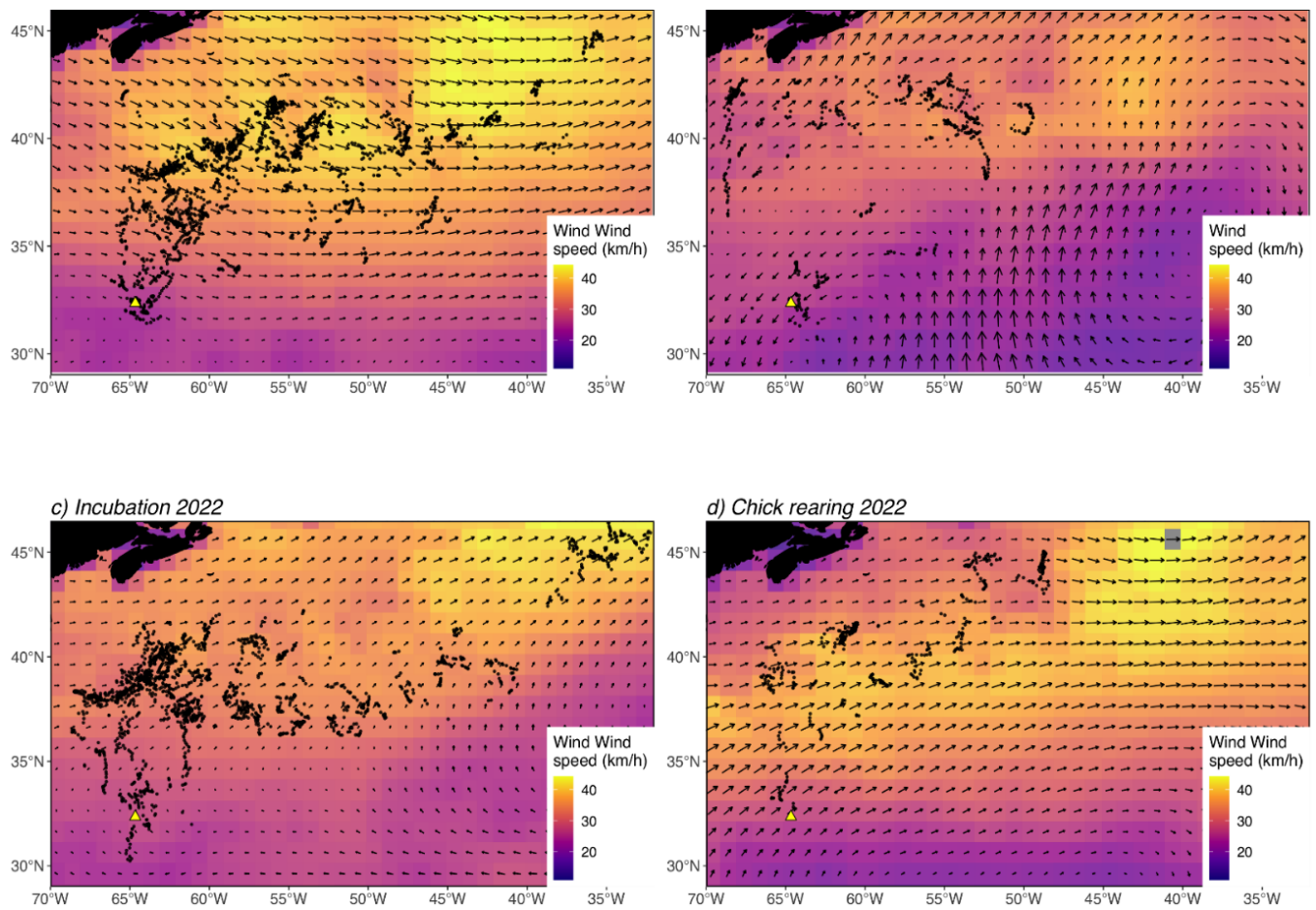
Fig. S14. Bermuda petrel locations classifies as "search" by means HMM (see Methods for more details) overlaid to the layer representing wind climatology over the study period with mean wind speeds (kmh^{-1}) increasing from blue to yellow and wind directions indicated by arrows.

SUPPLEMENT 2
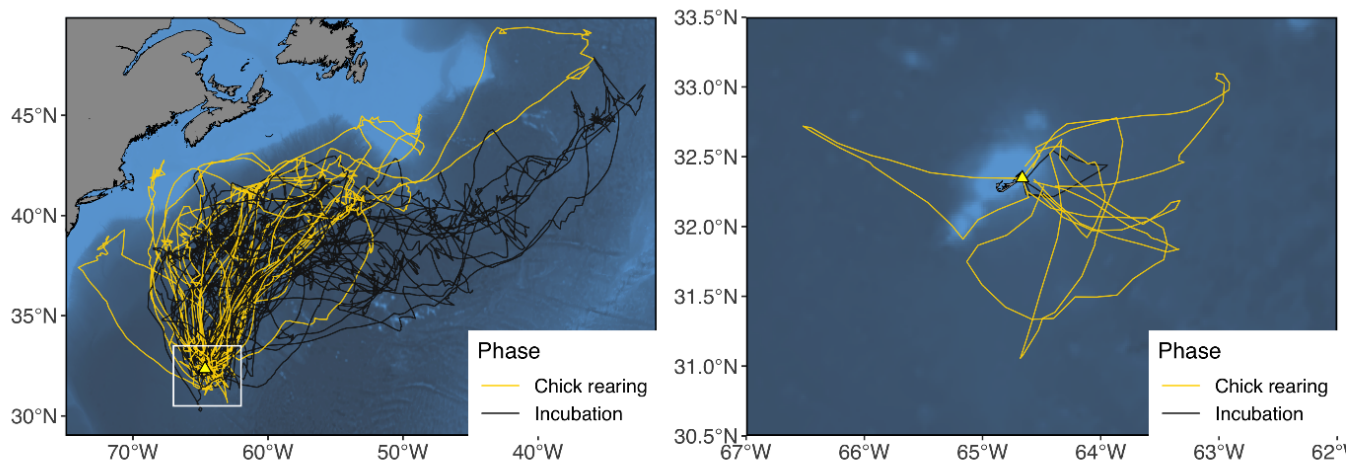
Fig. S15. Forty-five "long" foraging trips of Bermuda petrels (left panel) and 7 "short" trips (right panel; zoomed into area around colony) recorded during the breeding season 2019 and 2022. See Methods and Results for more details.
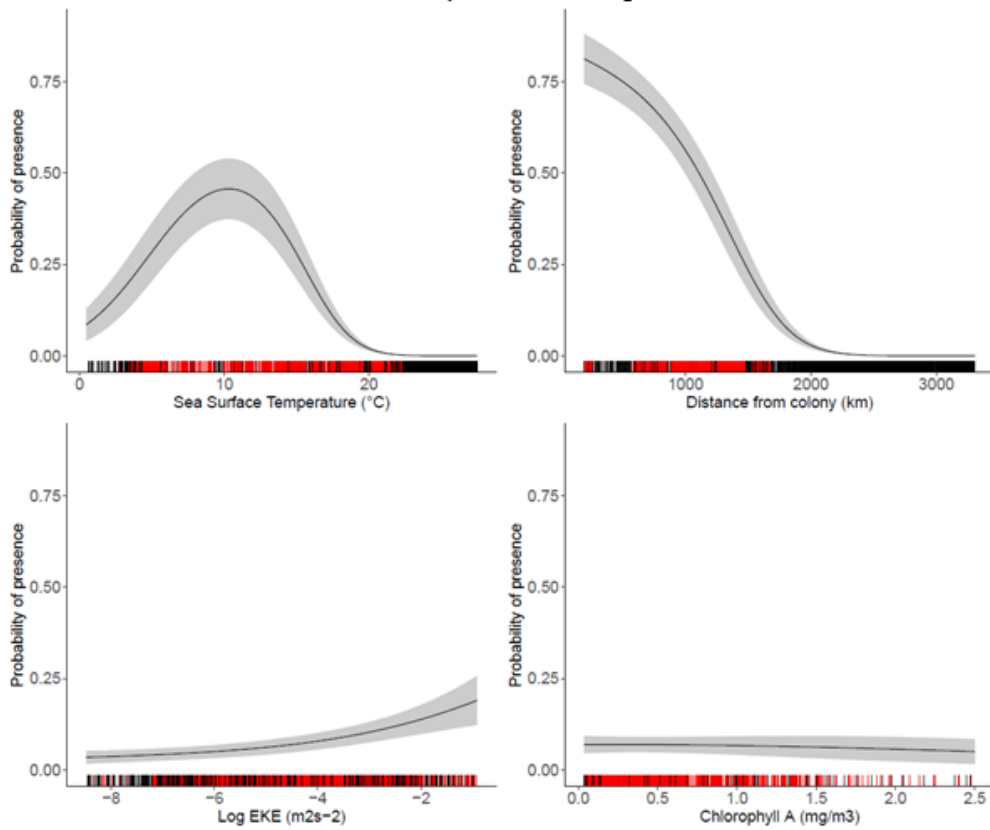

Fig. S16. Foraging areas of Bermuda petrels presented as 25%, 50 and 75% UDs (from dark to lighter colours) calculated by combining data from 2019 and 2022 breeding seasons and including only locations classified as "search" through HMM analysis (see Materials and Methods for more details).
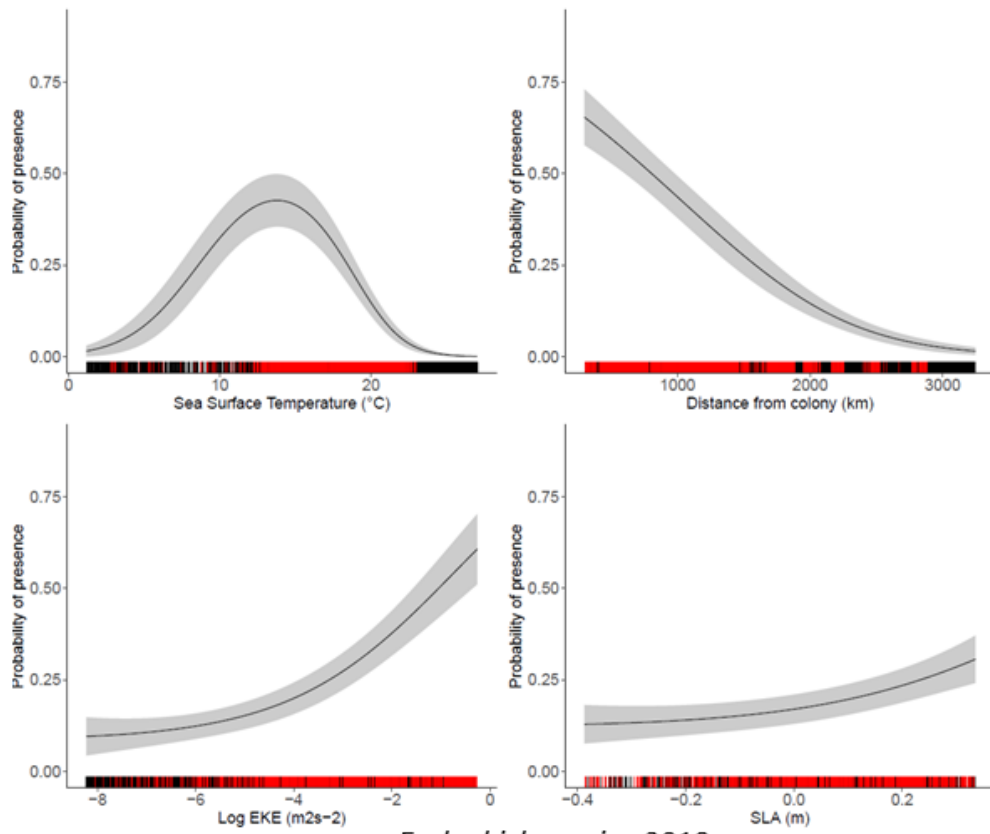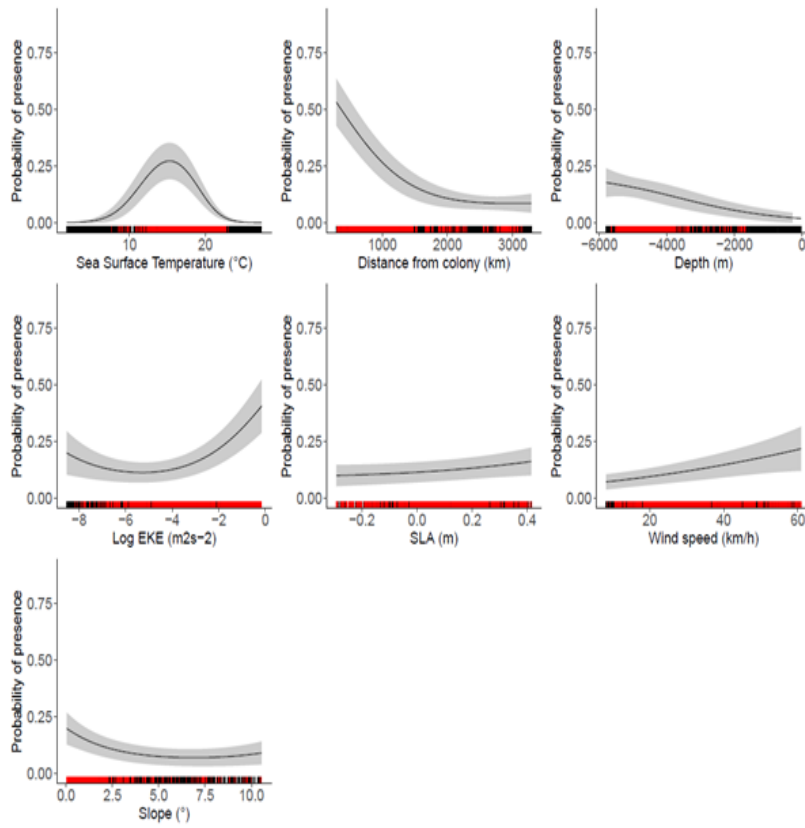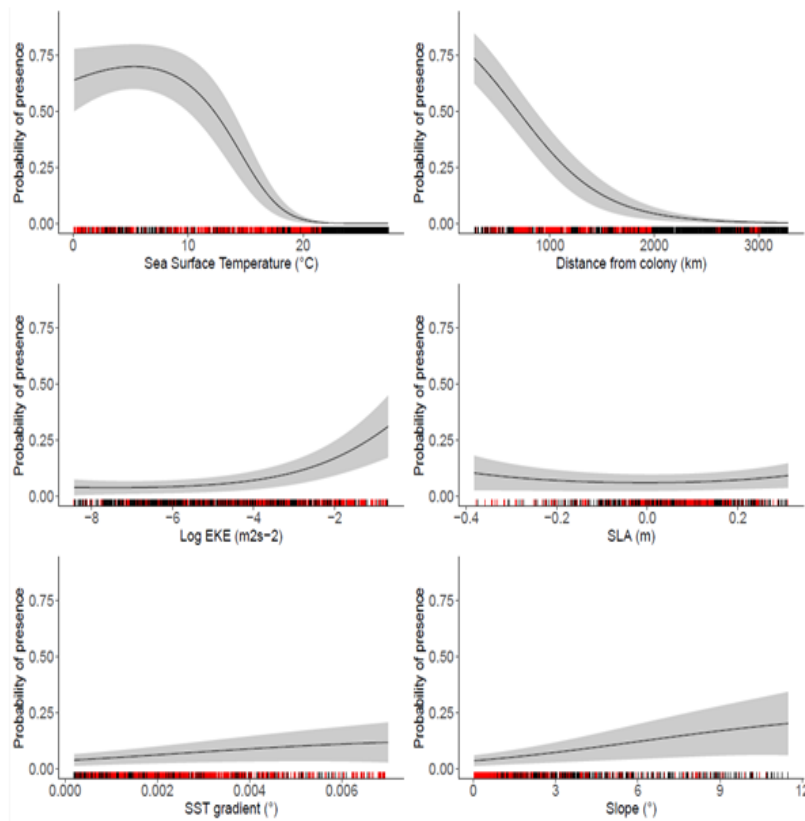
Fig. S17. Response curve of selected predictors for the Bermuda foraging habitat preference modelled separately for the incubation and early chick-rearing phases of 2019 and 2022 breeding seasons. Predictor variables included sea surface temperature, sea surface temperature gradient, sea level anomaly (SLA), chlorophyll A, distance to colony, log-transformed eddy kinetic energy (Log EKE), slope, depth and wind speed (see Methods and Table 2 for more details). Rug plots show the distribution of each predictor variable (black marks) while the red marks show predictor variable values for Y-presence data only.